



Synthesis, X-ray characterization and computational Studies of *N*-imidazolyl and *N*-pyrazolyl pyrimidine derivatives

Marta Torres^a, Pablo Cañellas^a, Carolina Estarellas^a, Angel García-Raso^{a,*}, Juan J. Fiol^a, Francisca M. Albertí^a, Antonio Frontera^{a,*}, Elies Molins^b, Ignasi Mata^b, Pere M. Deyà^a

^a *Departament de Química, Universitat de les Illes Balears, Crta. Valldemossa km 7.5, E-07122 Palma de Mallorca, Balears, Spain*

^b *Institut de Ciència dels Materials (CSIC), Campus de la Universitat Autònoma, E-0183 Cerdanyola del Vallès, Barcelona, Spain*

ARTICLE INFO

Article history:

Received 22 November 2011

Received in revised form 3 January 2012

Accepted 11 January 2012

Available online 24 January 2012

Keywords:

Pyrimidines

Imidazole and benzimidazole

Ab initio calculations

X-ray crystal structures

Anion– π interactions

ABSTRACT

In this manuscript we report the synthesis and X-ray characterization of neutral 2-(1*H*-imidazol-1-yl)-pyrimidine (**1**), 2-(1*H*-pyrazol-1-yl)-pyrimidine (**2**) and 1-(2-pyrimidinyl)-1*H*-benzimidazole (**3**). We have also obtained crystals of the corresponding hydrochlorides of compounds **1** and **3**. Finally, the outer sphere complex of protonated 2-(1*H*-imidazol-1-yl)-pyrimidine with [CoCl₄]²⁻ as counterion is described. In several charged structures interesting anion– π interactions determine the crystal packing. Moreover, in neutral systems some stacking interactions are governed by double lone pair– π interactions. High level ab initio calculations (RI-MP2/def2-TZVP) have been used to evaluate the non-covalent interactions observed in the solid state and the interplay between them.

© 2012 Elsevier Ltd. All rights reserved.

1. Introduction

For many years there has been great interest in the chemistry of pyrazoles, imidazoles, pyrimidines and related *N*-containing heterocyclic derivatives.^{1,2} Such systems play a significant role in many biological processes, due to their coordinating ability to metal ions.³ The chemistry of transition metals associated with polydentate ligands with sp² hybridised nitrogen atoms has been developed and very interesting inorganic architectures have been generated using this approach.⁴ In particular, ligands designed for this purpose consist of triazine or pyrimidine moieties attached to one or more pyrazol-1-yl substituents.⁵ These architectures are usually governed by a variety of noncovalent interactions.⁶ These forces include hydrogen-bonding,⁷ π – π stacking,⁸ cation– π ⁹ and C–H/ π ^{8b,10} contacts, which are very common and well accepted among the supramolecular chemists. For around ten years, a new type of supramolecular interaction, namely anion– π interaction,¹¹ has been increasingly reported in the literature, notwithstanding the preliminary improbability of considering repulsive interactions among the aromatic clouds and electron rich molecules.¹² The design of highly selective anion receptors and channels represent important advances in this nascent field of supramolecular

chemistry. Matile et al.¹³ have also published remarkable synthetic ion channels based on anion– π interactions. In addition, its important role in enzymatic processes has been recently described.¹⁴ The closely related lone pair (lp)– π interactions have been recently reviewed by Gamez et al.,¹⁵ designating the lone pair– π contacts as a new supramolecular bond and rigorous analysis of the Cambridge Structure Database revealed that such contacts are not unusual in organic compounds, but have been overlooked in the past. Egli et al. have studied the importance of lone pair– π interactions in bio-macromolecules (Z-DNA and RNA).¹⁶ Indeed, lone pair– π interactions have been found to be of great importance for the stabilization of biological macromolecules, as well as for the binding of inhibitors in the binding pocket of biochemical receptors.¹⁷

We have recently reported that protonated adenines and pyrimidines are well suited for establishing strong anion– π interactions with a variety of anions, including BF₄⁻, NO₃⁻, Cl⁻, ZnCl₄²⁻, etc.¹⁸ In this manuscript we report the synthesis of 2-(1*H*-imidazol-1-yl)-pyrimidine (imipyr, **1**), 2-(1*H*-pyrazol-1-yl)-pyrimidine (pyr-apyr, **2**) and 1-(2-pyrimidinyl)-1*H*-benzimidazole (bimipyr, **3**). Their molecular structures in the solid state have been elucidated by X-ray diffraction analysis. Furthermore, we also report the synthesis and X-ray characterization of the corresponding hydrochlorides of **1** and **3** (compounds **4** and **5**, respectively). Moreover, a multicomponent assembly has been characterized by X-ray crystallography (compound **6**), which consist in a co-crystal of **2** and the nitrate salt of protonated pyrimidin-2-one (see Fig. 1).

* Corresponding authors. Fax: +34 971 173426; e-mail addresses: angel.garcia-raso@uib.es (A. García-Raso), toni.frontera@uib.es (A. Frontera).

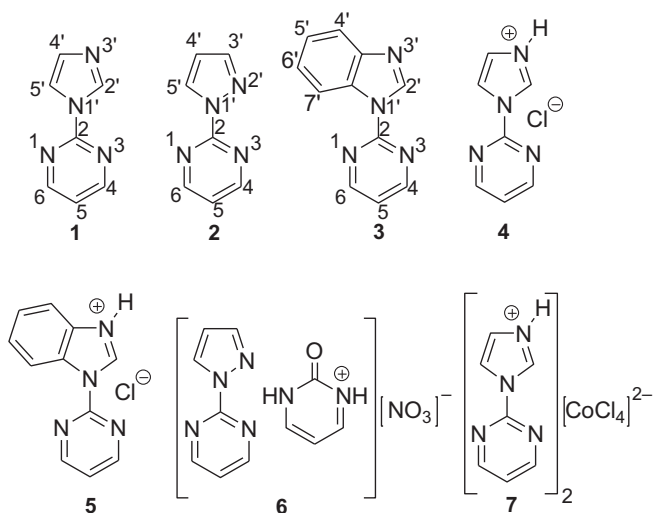


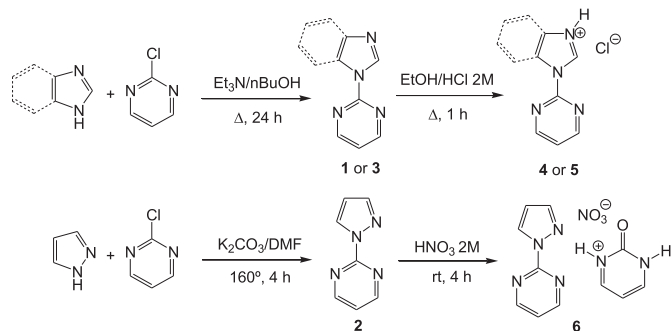
Fig. 1. Compounds 1–7 reported in this manuscript and the numbering scheme.

Finally, an outer sphere complex of protonated **1** with CoCl_4^{2-} is also reported (compound **7**). Latter complex and the hydrochloride salt of **1** exhibit interesting anion– π interactions in the solid state, which are important in the crystal packing. The neutral complexes **1–3** present different stacking modes that have been analyzed. The different noncovalent interactions observed in the solid state have been studied using high level ab initio calculations. The anion– π binding properties of the protonated 2-(1*H*-imidazol-1-yl)pyrimidine via hydrogen-bonding and anion– π interactions have been studied using the Molecular Interaction Potential with polarization (MIPp)¹⁹ calculations. The MIPp is a convenient tool for predicting binding properties. It has been successfully used for rationalizing molecular interactions, such as hydrogen bonding and ion– π interactions and for predicting molecular reactivity.²⁰

2. Results and discussion

2.1. Synthesis of the compounds

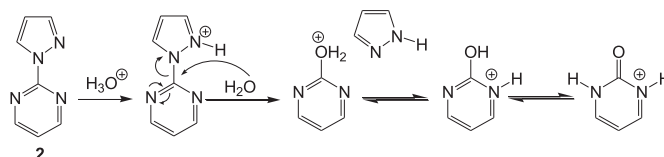
We have synthesized compounds **1–6** using our own developed methodology by means of the general procedure shown in Scheme 1. Compounds **1–3** are easily prepared, in acceptable yields (40–60%), from 2-chloropyrimidine and the corresponding (benzo) diazole under refluxing conditions in the presence of a base (K_2CO_3 or Et_3N). Dissolution of compound **1** or **3** in EtOH/HCl 2 M yields the corresponding salts, **4** and **5**, respectively.



Scheme 1. Synthetic route to compounds 1–6.

As can be seen in Scheme 1, although the corresponding hydrochloride derivatives of imidazole compounds have been easily

obtained by treatment of EtOH/HCl 2 M, intents to prepare the similar pyrazole hydrochloride have been unsuccessful, yielding always different mixtures of compound **2** and products derived from the C–N bond cleavage. In addition, when the reaction time was 24 h/ Δ the products detected by ^1H NMR spectroscopy were only pyrazole and protonated pyrimidinone. In a single experience at room temperature, 4 h, using HNO_3 2 M few crystals of the mixture **6** were obtained. A possible explanation of this particular reactivity of compound **2** is shown in Scheme 2, where a nucleophilic attack of a water molecule on C-2 by means of an addition–elimination mechanism yields the protonated pyrimidinone.



Scheme 2. Plausible mechanism of the unexpected formation of protonated pyrimidinone.

Finally, compound **7** was obtained by slow evaporation at 40 °C of a solution of **1** and CoCl_2 , yielding blue crystals suitable for X-ray analysis.

2.2. Crystal structure description of neutral compounds

Although compounds **1–3** were previously synthesized,²¹ their X-ray characterization is surprisingly missing in the literature. Actually, X-ray structures of derivatives of **1** and **3** either complexed to transition metals or alone are not found in the CSD. The ORTEP diagrams of compounds **1–3** are shown in Fig. 2. Compound **1** crystallizes in the triclinic crystal system and compounds **2** and **3** crystallize in the monoclinic crystal system. The crystallographic data collection and refinement parameters are listed in Table 1.

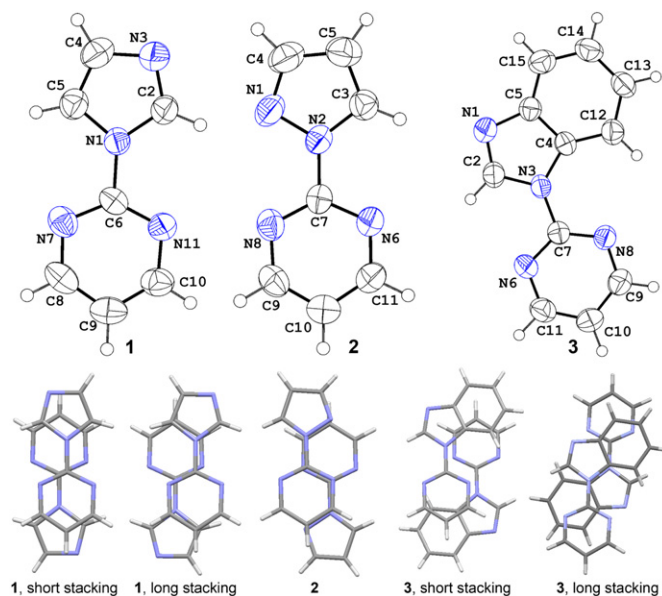


Fig. 2. Top: ORTEP diagrams of 1–3. The thermal ellipsoids are drawn at the 50% probability level. Bottom: stacking modes observed in compounds 1–3.

In solid state, compounds **1–3** basically present C–H \cdots N hydrogen bonds and π – π stacking interactions. The geometric parameters of the hydrogen bonds observed in compounds **1–3** are summarized in Table 2. Stacking interactions are characterized by an antiparallel orientation of the molecules and a small

Table 1
Crystal data, data collection and structure solution for crystallographically characterized complexes 1–7

	1	2	3	4	5	6	7
Formula	C ₇ H ₆ N ₄	C ₇ H ₆ N ₄	C ₁₁ H ₈ N ₄	C ₇ H ₉ ClN ₄ O	C ₁₁ H ₁₁ ClN ₄ O	C ₁₁ H ₁₁ N ₇ O ₄	C ₁₄ H ₁₄ Cl ₄ CoN ₈
M/g mol ⁻¹	146.16	146.16	196.21	200.63	250.79	305.27	495.06
Crystal system	Triclinic	Monoclinic	Monoclinic	Monoclinic	Triclinic	Monoclinic	Monoclinic
Space group	<i>P</i> -1	<i>P</i> 21/ <i>n</i>	<i>P</i> 21/ <i>n</i>	<i>P</i> 21/ <i>n</i>	<i>P</i> -1	<i>P</i> 21/ <i>c</i>	<i>P</i> 21/ <i>c</i>
<i>a</i> /Å	5.764(4)	6.137(4)	7.4280(10)	9.885(3)	7.197(4)	6.373(6)	22.515(9)
<i>b</i> /Å	7.069(6)	10.237(3)	17.837(7)	5.115(3)	9.637(2)	7.688(5)	7.293(4)
<i>c</i> /Å	8.840(7)	11.377(3)	7.546(2)	18.807(8)	9.750(2)	27.576(3)	12.458(8)
α (°)	81.01(4)	90	90	90	65.052(17)	90	90
β (°)	80.36(4)	100.25(5)	112.620(10)	98.90(3)	78.94(3)	93.91(3)	79.76(5)
γ (°)	78.35(3)	90	90	90	73.17(3)	90	90
<i>V</i> /Å ³	345.0(5)	703.3(5)	922.9(5)	939.5(7)	585.0(4)	1348.0(15)	2011.8(19)
<i>Z</i>	2	4	4	4	2	4	4
ρ_c /g cm ⁻³	1.403	1.380	1.412	1.418	1.423	1.504	1.635
Absorption							
μ /mm ⁻¹	0.094	0.092	0.091	0.373	0.315	0.119	1.401
Correction	Empirical	Empirical	Gaussian	None	Gaussian	Gaussian	Gaussian
Max. <i>T</i>	1.000	0.955	0.989	—	0.921	0.961	0.829
Min. <i>T</i>	0.751	0.806	0.939	—	0.847	0.9496	0.669
GOF of <i>F</i> ²	0.883	1.057	0.966	1.079	1.065	1.055	1.025
Final <i>R</i> indices [<i>I</i> >2 σ (<i>I</i>)]							
<i>R</i> ₁	0.0821	0.0431	0.0511	0.0391	0.0430	0.0424	0.0468
<i>wR</i> ₂	0.1606	0.1107	0.1102	0.1051	0.1246	0.0994	0.1079
<i>R</i> indices (all data)							
<i>R</i> ₁	0.2074	0.0591	0.0903	0.0494	0.0537	0.0680	0.0816
<i>wR</i> ₂	0.192	0.1177	0.1222	0.1092	0.1298	0.1124	0.1277

Table 2
Hydrogen bond data for compounds 1–3

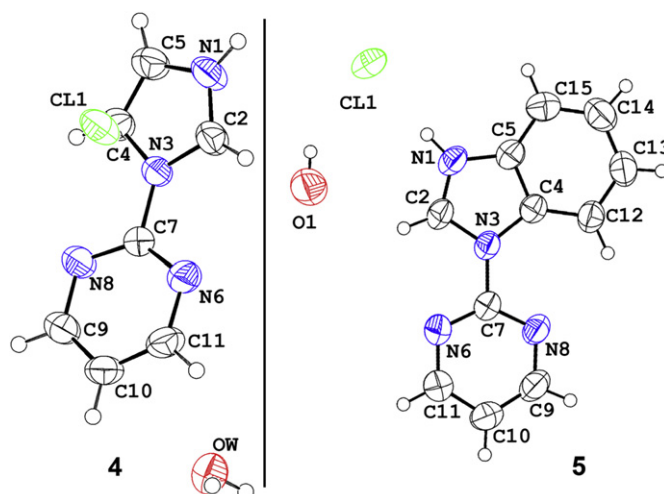
Label	X...Y (Å)	H...Y (Å)	X–H...Y (°)
Compound 1			
C2–H2...N6	3.370(6)	2.69	130(3)
C2–H2...N8	3.497(6)	2.75	137(3)
C4–H4...N1	3.761(7)	2.91	154(3)
C9–H9...N6	3.603(6)	2.94	129(3)
C10–H10...N1	3.532(6)	2.61	167(4)
Compound 2			
C3–H3...N6	3.518(3)	2.88	128(2)
C9–H9...N6	3.531(3)	2.68	152(2)
C3–H3...N8	3.567(3)	2.79	142(2)
C4–H4...N1	3.707(3)	2.80	158(2)
C10–H10...N6	3.599(3)	2.68	171(2)
Compound 3			
C2–H2...N6	3.319(3)	2.51	143(2)
C11–H11...N1	3.562(3)	2.73	143(2)
C10–H10...N1	3.538(3)	2.62	164(2)
C13–H13...N8	3.820(3)	2.91	162(2)
C12–H12...N8	3.008(3)	2.52	112(2)

superposition of the heterocycles when the stacking is projected in the molecular plane, see Fig. 2. These intermolecular interactions induce the formation of molecular ribbons or tapes, which are observed in the crystal structures (see Supplementary data for details).

2.3. Hydrochloride compounds 4 and 5

The ORTEP diagrams of the hydrochloride salts are shown in Fig. 3. Compounds 4 and 5 crystallize in the monoclinic and triclinic crystal system, respectively. Selected bond lengths, angles and supramolecular interactions are listed in Table 3 and crystallographic data collection and refinement parameters are listed in Table 1.

The hydrated salts 4 and 5 forms ribbons along (010) and (001), respectively, similar to those observed in 3. In compound 4, each protonated 2-(1*H*-imidazol-1-yl)-pyrimidine is connected to two antiparallel molecules by hydrogen bonding and stacking interactions (see Supplementary data for details). In addition, chlorides are situated over the imidazoles, at the side not involved in stacking, building an interesting anion– π/π – π/π –anion assembly (see Fig. 4, left), which will be further studied below. Moreover,

**Fig. 3.** ORTEP diagrams of 4 and 5. The thermal ellipsoids are drawn at the 50% probability level.**Table 3**
Hydrogen bond data in compounds 4 and 5

Label	X...Y (Å)	H...Y (Å)	X–H...Y (°)
Compound 4			
C4–H4...N8	3.405(3)	2.52	157(2)
N1–H1...Cl1	3.045(2)	2.20	162(2)
C2–H2...Cl1	3.398(3)	2.57	147(2)
Ow–Hw2...Ow	2.824(2)	1.98	174(3)
Ow–Hw1...Cl1	3.132(2)	2.28	172(3)
C5–H5...Ow	3.439(3)	2.52	163(2)
C9–H9...Ow	3.361(3)	2.60	137(2)
C11–H11...Cl1	3.575(2)	2.89	131(2)
Compound 5			
C11–H11...N6	2.523(2)	3.34	145(2)
O1–H1A...Cl1	2.530(4)	3.28	149(4)
O1–H1B...Cl1	2.330(4)	3.26	173(3)
N1–H1...Cl1	2.181(2)	3.05	173(3)
C2–H2...O1	2.536(2)	3.23	131(2)
C10–H10...O1	2.610(2)	3.31	133(2)
C14–H14...Cl1	2.925(2)	3.74	148(2)

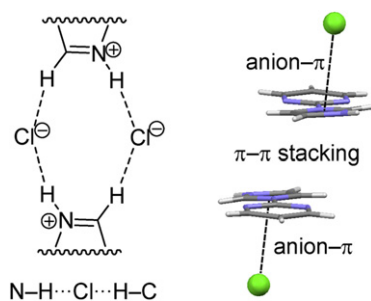


Fig. 4. Double hydrogen bonding (left) and anion- π / π - π / π -anion assembly (right) observed in compound **4**.

apart from the C-H...N hydrogen bonds observed in the neutral compounds a network of hydrogen bonds involving two 2-(1*H*-imidazol-1-yl)-pyrimidine molecules and two Cl⁻ atoms is observed (see Fig. 4, left). A similar supramolecular organization has been recently observed by Domasevitch and collaborators in bipyrazolium salts, which is originated by strong hydrogen bonding between multiple NH cationic donors and O, F, Cl, I anionic acceptors.²²

2.4. Compound 6

In an effort to obtain the solid state structure of a salt of compound **2**, we have tried several strategies, using a variety of acidic conditions. However, in sharp contrast to compounds **1** and **3**, it has been impossible to obtain the corresponding salt of **2**. In one of these attempts, using nitric acid, we have obtained an unexpected compound, which is a co-crystal of **2** and the nitrate salt of pyrimidin-2-one (see Fig. 5).

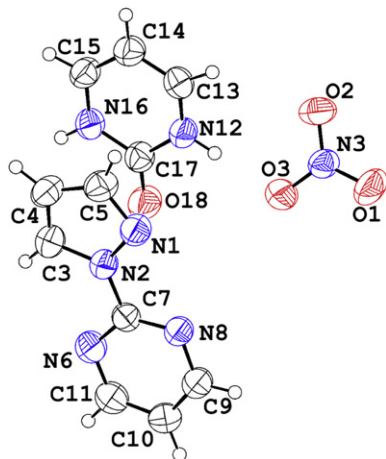


Fig. 5. ORTEP diagrams of **6**. The thermal ellipsoids are drawn at the 50% probability level.

In the solid state architecture of compound **6** we have found an interesting anion- π / π - π supramolecular assembly, where the protonated pyrimidin-2-one interacts simultaneously with nitrate anion at one side of the ring and with the pyrazol ring of **2** at the opposite side (see Fig. 6). The intermolecular distances observed for the anion- π and π - π are short (3.33 and 3.35 Å, respectively) indicating that the interactions are strong, which is due to the cationic nature of the protonated pyrimidin-2-one ring, which reinforces both interactions due to electrostatic effects.

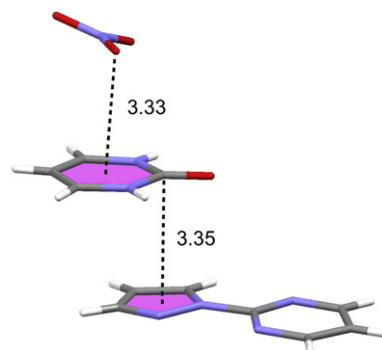


Fig. 6. X-ray crystallographic fragment of compound **6** with indication of the anion- π / π - π assembly. Distances in Å.

2.5. CoCl₄²⁻ complex 7

The ORTEP diagram of compound **7**, which crystallizes in the monoclinic crystal system, is shown in Fig. 7. Selected bond lengths, angles and supramolecular interactions are listed in Table 4 and crystallographic data collection and refinement parameters are listed in Table 1.

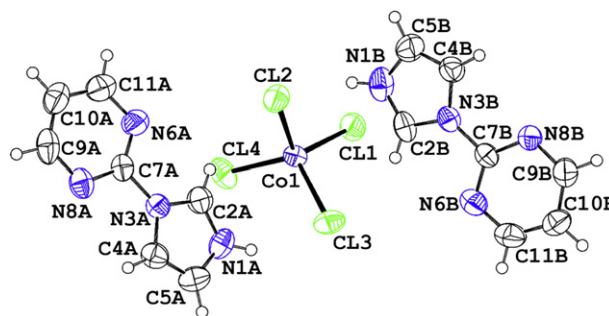


Fig. 7. ORTEP diagrams of **7**. The thermal ellipsoids are drawn at the 50% probability level.

Table 4
Hydrogen bond data in compound **7**

Label	X...Y (Å)	H...Y (Å)	X-H...Y (°)
C4B-H4B...N6B	3.591(6)	2.73	155(4)
C11B-H11B...N8B	3.594(7)	2.71	159(4)
C4A-H4A...N6A	3.702(7)	2.87	151(4)
C11A-H11A...N8A	3.786(7)	3.09	133(4)
N1A-H1A...Cl3	3.312(4)	2.54	140(4)
C2A-H2A...Cl2	3.585(5)	2.72	156(4)
N1B-H2B...Cl2	3.082(4)	2.26	166(5)
C2B-H2B...Cl3	3.699(5)	2.86	152(4)
C10A-H10A...Cl2	3.448(5)	2.70	137(4)
C5A-H5A...Cl1	3.343(5)	2.72	126(4)
C9B-H9B...Cl1	3.452(5)	2.80	128(4)
C10B-H10B...Cl3	3.736(5)	2.88	156(4)

The asymmetric unit in compound **7** consists of one CoCl₄²⁻ anion and two symmetry independent and protonated 2-(1*H*-imidazol-1-yl)-pyrimidine molecules (A and B) in antiparallel conformation. In the crystal structure, each one of these molecules forms layers parallel to the (100) plane, being CoCl₄²⁻ intercalated between these layers (Fig. 8). Thus, the succession of layers along (100) consists of A, CoCl₄²⁻, B, CoCl₄²⁻. Molecule B layers are formed by corrugated tapes (angle between molecular planes 46.4°) along (001), being the pyrimidine of one molecule connected to the next by two C-H...N hydrogen bonds. The shorter stacking (3.337 Å) is part of an interesting anion- π / π - π / π -anion assembly involving two

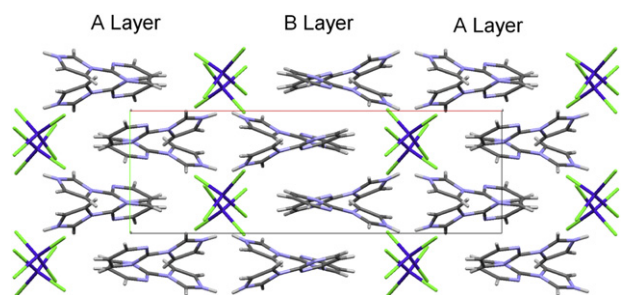


Fig. 8. Top: Crystal packing along (100) in compound **7**, with indication of the layers that are perpendicular to the horizontal and parallel to the vertical directions.

CoCl_4^{2-} in different layers, with the Cl atoms over the imidazole rings (3.144 Å). One of these assemblies (for B molecule) is highlighted in Fig. 9. The distances are measured from the ring centroid to the closest chlorine atom of the anion.

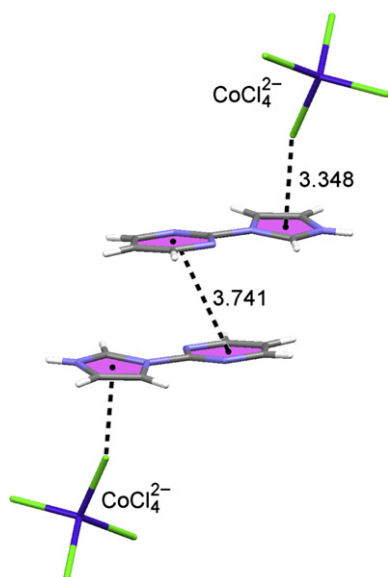


Fig. 9. Anion- π - π -anion assembly observed in the crystal packing along of **7**. Distances in Å.

2.6. Theoretical ab initio study

We have divided this section into two parts. First we focused our study in the stacking features of the neutral compounds, including a comparison with similar compounds found in the CSD. Second, we study the energetic characteristics of the anion- π and H-bonding interactions found in two charged compounds and their mutual influence.

2.6.1. Neutral compounds. First we have analyzed the energetic features of the stacked dimers observed in the solid state of compounds **1**–**3** (see Fig. 3). In Table 5 we summarize the binding energies and distances of several dimers. It can be observed that dimer **3** is the most favourable probably because it has a more extended π -system. Both stacking modes observed in **1** are also very favourable. In **1** (long stacking) there is a very small superposition of the π systems, however it can be observed that the nitrogen atoms are exactly over the carbon atoms and vice versa, maximizing the electrostatic interactions and giving stability to the complex. In **1** (short stacking) there is a higher superposition of the π systems. As aforementioned, this dimer can be also viewed as a special stacking arrangement, where two lp- π interactions are

Table 5

Interaction energies without and with the basis set superposition error (E and E_{BSSE} , respectively, in kcal/mol) and distances (R , Å) of several dimers at RI-MP2/def2-TZVP level of theory

Dimer	E	E_{BSSE}	R
1 , Short stack.	-13.9	-11.4	3.40
1 , Long stack.	-15.2	-12.7	3.55
2	-13.1	-10.7	3.47
3 , Short stack.	-18.8	-15.2	3.40
3 , Long stack.	-18.2	-14.6	3.53
CEWVOQ	-12.1	-9.5	3.35
TIGLUR	-7.2	-5.1	3.24
YOLXAZ	-12.6	-9.5	3.24

established. We have examined the CSD searching related compounds to learn if this binding mode is also present in other structures. We have searched fragments consisting in a pyrimidine molecule with either an imidazo-1-yl or a pyrazo-1-yl substituent in position **2**. Other restrictions have not been imposed. There are only 37 structures in the database and all of them correspond to 2-(1*H*-pyrazol-1-yl)-pyrimidine derivatives. Therefore the X-ray structures of 2-(1*H*-imidazol-1-yl)-pyrimidine derivatives reported herein are unprecedented in the CSD. Most of the 37 structures are metal complexes and only 13 structures correspond to neutral molecules. In some of them we have found stacking interactions that present the double lp- π binding mode. Some selected examples are shown in Fig. 10. We have computed the interaction energies of the dimers of CEWVOQ,²³ TIGLUR²⁴ and YOLXAZ.²⁵ We have used models where the substituents have been replaced by hydrogen atoms, in order to study the stacking energies free from other influences. The interaction energies are also included in Table 5. The stacking mode observed for **1** is slightly more favourable than the observed in CEWVOQ and YOLXAZ. The TIGLUR presents the least favourable interaction energy.

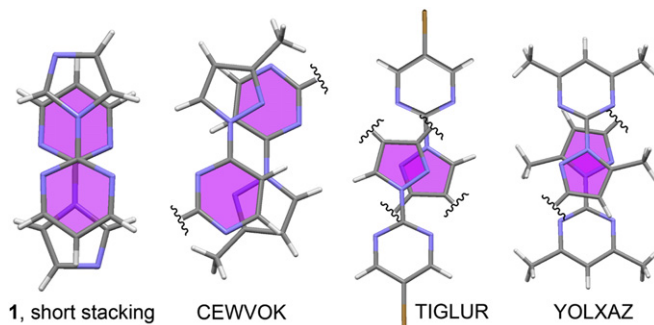


Fig. 10. On top representation of X-ray structures showing double lp- π interactions.

We have also studied the energetic features of the hydrogen bonded dimers observed in the solid state in compounds **1** and **3**, where four C-H...N H-bonds are formed using a different combination of hydrogen bonds (see Fig. 11). The interaction energies of both dimers are gathered in Table 6. It can be observed that the interaction energy of compound **3** is 1 kcal/mol more favourable than compound **1**, in agreement with the H-bonding distances. In fact compound **1** exhibits a very long H-bond distance in one C-H...N bond (2.99 Å). We have also computed the distribution of critical points (CP) using the Bader's theory of 'atoms in molecules'. Both dimers are characterized by the presence of four bond CPs connecting the hydrogen atoms with the nitrogen atoms. As a consequence two ring CPs raise. The values of the charge density at the ring CPs are also included in Table 6. It can be appreciated that the value at the ring CP in dimer **3** is greater than **1**, in agreement with the interaction energies.

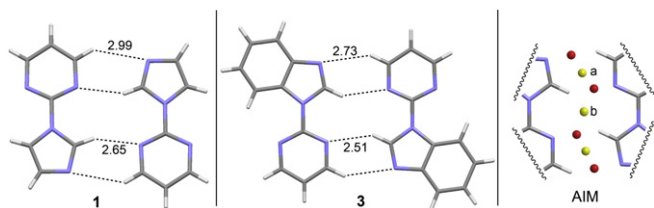


Fig. 11. H-bonded dimers of **1** and **3**. Right: bond (red) and ring (yellow) critical points distribution in **1** and **3**.

Table 6

Interaction energies without and with the basis set superposition error (E and E_{BSSE} , respectively, in kcal/mol) and distances (R , Å) of H-bonded dimers **1** and **3** at RI-MP2/def2-TZVP level of theory. The values of the charge density at the ring critical points (RCP) are also included in au

Dimer	E	E_{BSSE}	R	ρ_{RCP} (a)	ρ_{RCP} (b)
1	-8.28	-7.20	2.65/2.99	0.1604	0.2438
3	-9.35	-8.10	2.51/2.73	0.2413	0.3558

2.6.2. Charged compounds. From the X-ray analysis of **4**, an interesting anion- $\pi/\pi-\pi/\pi$ -anion- π assembly (see Fig. 4, right) has been observed, that is, very important in determining the solid state structure of this compound. We have first studied if the position of the anion over the ring is dominated by the anion- π interaction or, on the contrary, it is due to the other interactions established by the anion. To shed light to this question, we have computed the Molecular Interaction Potential with polarization (MIPp) of a crystal fragment consisting of a H-bonded dimer of the protonated 2-(1*H*-imidazol-1-yl)-pyrimidine moiety interacting with two chloride anions in order to have a neutral system (see Fig. 12). We have computed the bidimensional (2D) energy map of this fragment interacting with chloride at 3.0 Å above the molecular plane in order to study the spatial regions where the π -interaction with Cl^- is more favourable. The 2D-MIPp map computed for the interaction of a fragment of **4** with Cl^- is shown in Fig. 12. It can be observed that there is a wide region where the lowest interaction potential isocontour line is located (red line). It can be appreciated the location of the chloride anion in the crystal structure (see Fig. 4 and the on-top representation in the top-left corner of Fig. 12) coincides with the lowest isocontour line. This result gives reliability

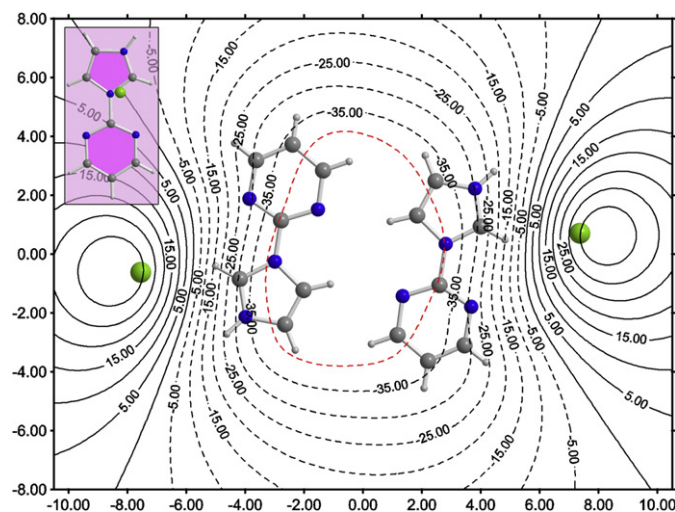


Fig. 12. 2D-MIPp(Cl^-) energy map of **4** at a plane located at 3.0 Å above the molecular plane. Isocontour lines are drawn ever 5 kcal/mol apart from the lowest isocontour line (red line, -39 kcal/mol). Positive values of potential are represented by solid lines and negative values by dashed lines.

to the MIPp method and indicates that the position of the anion in the crystal structure depends on this interaction and probably the final position over this contour line comes from the other non-covalent forces. The lowest isocontour line observed in the 2D-MIPp map reflects a very flat potential surface. This fact agrees with the experimental results and the Hirshfeld surfaces (see Supplementary data) that indicate the unidirectionality of the anion- π interaction in compound **4**.

We have also analyzed the influence of the formation of the hydrogen bonded dimer on the anion- π interaction. We have first computed the interaction energy of the anion- π complex where only one protonated 2-(1*H*-imidazol-1-yl)-pyrimidine is present (**4A**, see Fig. 13). Secondly, we have computed the interaction energy in complex **4B** where the hydrogen bonded dimer interacts with the chloride anion. The computed interaction energies are gathered in Table 7 (first and second columns). The anion- π interaction energy (E_{BSSE}) computed considering that the dimer (interacting with the chloride ions located at the molecular plane) has been previously formed (**4B**) is almost 10 kcal/mol more favourable than the anion- π interaction considering only the monomer (**4A**), indicating that the presence of the double C-H \cdots N hydrogen bond strengthens the anion- π interaction. We also include in Table 7 the energetic results obtained with the MIPp method for the two systems considered, which are in reasonably agreement with the E values obtained at the RI-MP2/def2-TZVP level of theory. Taking advantage of the MIPp method that gives an intuitive partition of the total interaction energy (E_t) into three components (see computational details), we have studied the physical nature of the anion- π interaction to know, which term is responsible of the strengthening of the interaction by the presence of the hydrogen bonds. It can be observed that the polarization and van der Waals terms (E_p and E_{VW} , respectively) are similar in **4A** and **4B**. In addition in **4A** the total interaction energy is dominated by the electrostatic (E_e) and E_p terms. In contrast, in **4B** the electrostatic term is very important and clearly dominates the interaction and it is the responsible of the strengthening of the interaction.

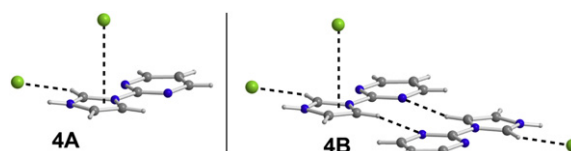


Fig. 13. Anion- π complexes **4A** and **4B**.

Table 7

Interaction energies (kcal/mol) and distances (R , Å) of H-bonded dimers **4A** and **4B** at RI-MP2/def2-TZVP level of theory. The values of the MIPp terms in kcal/mol are also included

Complex	E	E_{BSSE}	E_e	E_p	E_{VW}	E_t
4A	-22.3	-20.1	-11.1	-9.7	-1.5	-22.3
4B	-33.4	-29.7	-24.8	-10.7	-1.6	-37.1

Finally, we have studied computationally the noncovalent interactions observed in compound **7**, focussing the analysis in the influence of the hydrogen bonding interactions upon the anion- π interactions. Both interactions are crucial in the crystal packing of **7**. In fact the CoCl_4^{2-} anion is stabilized by two double $\text{Cl}^- \cdots \text{H}-\text{N}$ and $\text{Cl}^- \cdots \text{H}-\text{C}$ hydrogen bonds and two anion- π interactions (see Fig. 14, bottom right). As expected the $\text{Cl}^- \cdots \text{H}-\text{N}$ hydrogen bonds are shorter than the $\text{Cl}^- \cdots \text{H}-\text{C}$ ones. The anion- π distances are slightly different and both are established by means of the five-membered ring. We have evaluated the interaction energy of the anion- π contacts using two equations (see Fig. 14) in order to

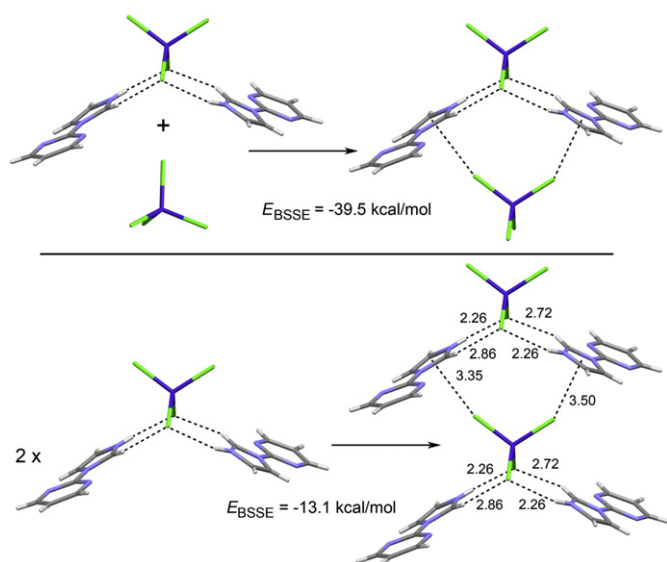


Fig. 14. Several fragments of the crystal structure of compound **7** and the reactions used to evaluate the anion– π interaction. Distances in Å.

evaluate the influence of the hydrogen bonds. We have first computed the anion– π interaction energy between a neutral fragment of the crystal structure and CoCl_4^{2-} (Fig. 14, top). The interaction energy of this assembly is -39.5 kcal/mol. This value is probably overestimated, since the anion is also interacting via hydrogen bonding to other two protonated 2-(1*H*-imidazol-1-yl)-pyrimidine moieties. When the anion– π interaction is evaluated using a second model where both interacting parts are uncharged (see Fig. 14, bottom) the binding energy is reduced to -13.10 kcal/mol. Therefore the consideration of the ‘naked’ anion in the calculations overestimates the interaction energy. The intricate combination of hydrogen bonding, anion– π and π – π stacking interactions is responsible of the unexpected 3D architecture observed in the solid state of this interesting structure.

3. Conclusions

To conclude, we have synthesized and X-ray characterized several imidazolyl, pyrazolyl and benzimidazolyl derivatives of pyrimidine that illustrate the importance of anion– π , π – π and hydrogen bonding interactions in supramolecular chemistry. Moreover, we have evaluated the energy of several noncovalent interactions involved in the crystal structure architecture of the compounds by using high level ab initio calculations. In addition, the 2D-MIPp energy maps are in good agreement with the X-ray structures, since they are able to predict the spatial regions where the interaction of the anion with the ring is more favourable. Using MIPp calculation we have also studied the influence of the hydrogen bonded dimers on the anion– π interactions in compound **1**. Interestingly, the partition of the energy indicates that electrostatic effects are responsible of the anion– π enhancement. Finally, in-depth understanding of weak intermolecular forces that govern crystal packing potentially allows a rational design of solids with tailored physical and chemical properties. The results described above are certainly of importance in this regard and helps to gain knowledge in this emerging area of supramolecular chemistry.

4. Experimental section

4.1. Material and measurements

Chemicals and solvents were purchased from commercial sources (Sigma and Aldrich) and were used as received. Elemental

analyses were carried out using Carlo-Erba models 1106 and 1108 and Thermo Finigan Flash 1112 microanalysers. Infrared spectra (KBr pellets) were recorded on a Bruker AMX 300 spectrometer. Proton and carbon chemical shifts in dimethyl sulfoxide solution ($\text{DMSO-}d_6$) were referenced to $\text{DMSO-}d_6$ itself [$^1\text{H NMR}$, $\delta(\text{DMSO})=2.50$; $^{13}\text{C NMR}$ $\delta(\text{DMSO})=39.5$ ppm]. Thermogravimetric data in the temperature range from 30 to 700 °C were recorded in a flowing air atmosphere (heating rate 5 °C min^{-1}) on a TA Instruments SDT 2960 Simultaneous DSC-TGA thermobalance.

4.2. Preparation of the compounds

4.2.1. 2-(1*H*-Imidazol-1-yl)-pyrimidine (1). A suspension of 2-chloropyrimidine (1.15 g, 9.5 mmol) and 0.65 g of imidazole (9.5 mmol) in *n*-butanol (20 ml) and triethylamine (2 ml) were heated (vigorous reflux) using an external oil bath at 160 °C during 24 h. While the reaction is going on the orange suspension is transformed into a brown solution. After standing and cooling the solution, precipitation of triethylammonium hydrochloride may occur. In this case, the precipitate was filtered off. In any case, the resulting solution was evaporated to dryness and the resulting solid washed with cold water and dried (60%). Recrystallisation from diethyl ether yield white monocrystals. (Found: C: 56.27; H: 4.46; N: 36.11%. Calcd for $\text{C}_7\text{H}_6\text{N}_4 \cdot 0.33(\text{H}_2\text{O})$ C: 56.26; H: 4.42; N: 36.82%). IR (cm^{-1}): 1577s, 1570s, 1480s, 1446s, 1333m, 1092w, 1053m, 791m, 751m, 650m, 635m, 618w, 515w, 482m. $^1\text{H NMR}$, $\delta(300 \text{ MHz; DMSO-}d_6)$: 8.85d [2H, $J=4.8$ Hz; C4-H, C6-H], 8.56s [1H, C2'-H], 7.93s [1H, C5'-H], 7.43t [1H, $J=4.8$ Hz, C5-H], 7.13s [1H, C4'-H]. $^{13}\text{C NMR}$ $\delta(75 \text{ MHz; DMSO-}d_6)$: 160.1 [C6, C4], 154.4 [C2], 136.1 [C2'], 131.0 [C4'], 120.3 [C5], 117.2 [C5'] (see Fig. 1 for the numbering scheme).

4.2.2. 2-(1*H*-Pyrazol-1-yl)-pyrimidine (2). Anhydrous K_2CO_3 (1.39 g, 10 mmol) was added to a solution of pyrazole (0.68 g, 10.0 mmol) in 15 ml of DMF and stirred at room temperature during 15 min. 2-Chloropyrimidine (1.15 g, 10.0 mmol) was added and the suspension refluxed during 24 h. The resulting solids were filtered off at room temperature to remove the impurities and the mother solution was evaporated in vacuum to yield a syrup, which is extracted with diethyl ether (3 \times 20 ml) and after, newly, evaporated in vacuum. The resulting oil was, finally, purified by flash chromatography ($\text{CHCl}_3/\text{SiO}_2$). A white solid (0.58 g, 40%) is obtained by evaporation of the solvent. (Found: C: 57.32; H: 4.16; N: 38.20%. Calcd for $\text{C}_7\text{H}_6\text{N}_4$ C: 57.53; H: 4.14; N: 38.34%). IR (cm^{-1}): 1569s, 1523m, 1558s, 1435s, 1400s, 1346m, 1309m, 1261m, 1217m, 1192m, 1146m, 1074w, 1051m, 1035m, 989m, 931s, 910m, 863w, 826m, 791m, 767m, 736m, 650m, 633m, 609m, 541m, 476m. $^1\text{H NMR}$, $\delta(300 \text{ MHz; DMSO-}d_6)$: 8.91d [2H, $J=4.8$ Hz; C4-H, C6-H], 8.70d [1H, $J=7.8$ Hz; C5'-H], 7.91br s [1H, C3'-H], 7.52t [1H, $J=4.8$ Hz; C5-H], 6.65br s [1H, C4'-H]. $^{13}\text{C NMR}$ $\delta(75 \text{ MHz; DMSO-}d_6)$: 159.8 [C6, C4], 155.8 [C2], 143.8 [C3'], 129.9 [C5'], 120.0 [C5], 109.2 [C4'].

4.2.3. 2-(1*H*-Benzimidazol-1-yl)-pyrimidine (3). A suspension of 2-chloropyrimidine (0.58 g, 5 mmol) and 0.61 g of benzimidazole (5 mmol) in *n*-butanol (10 ml) and triethylamine (1 ml) were heated (vigorous reflux) using an external oil bath at 160 °C during 24 h. The initial orange suspension is transformed into a brown solution. After standing and cooling the solution, precipitation of triethylammonium hydrochloride was obtained, which was filtered off. The resulting solution was evaporated in vacuum to dryness and the resulting solid washed with cold water and vacuum dried (40%). (Found: C: 67.16; H: 4.12; N: 28.63%. Calcd for $\text{C}_{11}\text{H}_8\text{N}_4$ C: 67.34; H: 4.11; N: 28.55%). IR (cm^{-1}): 1570s, 1498s, 1464s, 1440s, 1431s, 1320s, 1299s, 1248s, 1204s, 1003w, 888m, 830s, 793s, 766s, 742s, 640m, 583m, 510m, 424m. $^1\text{H NMR}$, $\delta(300 \text{ MHz; DMSO-}d_6)$: 9.08s [1H, C2'-H], 8.93d [2H, $J=4.8$ Hz; C4-H, C6-H], 8.53d [1H,

$J=7.8$ Hz; C4'-H], 7.76d [1H, $J=7.8$ Hz; C7'-H], 7.48t [1H, $J=4.8$ Hz; C5-H], 7.41t [1H, $J=7.8$ Hz, C5'-H], 7.34t [1H, $J=7.8$ Hz, C6'-H].

4.2.4. 2-(1H-Imidazol-1-yl)-pyrimidine hydrochloride monohydrate (4). Dissolution of (1) in EtOH/HCl 2 M yields the corresponding salt as suitable crystals for X-ray diffraction. (Found: C: 41.89; H: 4.41; N: 27.73%. Calcd for $C_7H_7N_4Cl \cdot H_2O$ C: 41.91; H: 4.52; N: 27.53%). IR (cm^{-1}): 1630w, 1590s, 1566m, 1530s, 1421s, 1353m, 1128w, 1043m, 969w, 833m, 791m, 768s, 737m, 633s, 508w, 482m, 418s, 386w. 1H NMR, δ (300 MHz; DMSO- d_6): 9.70s [1H, C2'-H], 8.98d [2H, $J=4.8$ Hz; C4-H, C6-H], 8.31s [1H, C5'-H], 7.72s [1H, C4'-H], 7.68t [1H, $J=4.8$ Hz, C5-H]. ^{13}C NMR δ (75 MHz; DMSO- d_6): 160.4 [C6, C4], 153.0 [C2], 135.5 [C2'], 122.6 [C5, C5'], 119.12 [C4'].

4.2.5. 2-(1H-Benzimidazol-1-yl)-pyrimidine hydrochloride $\cdot 1.3H_2O$ (5). A solution of 60 mg of (3) in 12 ml of HCl 2 M in EtOH was refluxed during 30 min. Evaporation of the final solution at room temperature yields the corresponding crystals (40%). (Found: C: 51.55; H: 4.29; N: 21.65%. Calcd for $C_{11}H_9ClN_4 \cdot 1.3H_2O$ C: 51.59; H: 4.57; N: 21.88%). IR (cm^{-1}): 1637w, 1619m, 1528m, 1449s, 1391s, 1272w, 1232m, 1004w, 938w, 800m, 755s, 621m, 601m, 538w, 416m. 1H NMR, δ (300 MHz; DMSO- d_6): 9.66s [1H, C2'-H], 8.99d [2H, $J=4.8$ Hz; C4-H, C6-H], 8.60d [1H, $J=7.8$ Hz, C4'-H], 7.84d [1H, $J=7.8$ Hz; C7'-H], 7.58t [1H, $J=4.8$ Hz; C5-H], 7.53t [1H, $J=7.8$ Hz, C5'-H], 7.49t [1H, $J=7.8$ Hz, C6'-H]. ^{13}C NMR δ (75 MHz; DMSO- d_6): 160.0 [C6, C4]; 155.5 [C2], 142.4 [C2'], 140.2 [C8'], 126.1 [C9'], 120.5 [C5], 118.7 [C7'], 116.5 [C4'].

4.2.6. Mixture of 2-(1H-pyrazol-1-yl)-pyrimidine and protonated pyrimidinone nitrate (1:1)(6). A solution of 63 mg (4.3 mmol) of (2) in 10 ml of HNO_3 2 M was stirred at room temperature during 4 h. Slow evaporation at room temperature yield two single crystals, suitable for X-ray diffraction, which correspond to the mixture (6). 1H NMR, δ (300 MHz; DMSO- d_6): 8.91d [2H, $J=4.8$ Hz; C4-H, C6-H], 8.71br d [2H, C4-H, C6-H protonated pyrimidinone and C5'-H], 7.91br s [1H, C3'-H], 7.52t [1H, $J=4.8$ Hz; C5-H], 6.78t [1H, $J=4.8$ Hz; C5-H protonated pyrimidinone], 6.65br s [1H, C4'-H].

4.2.7. 2-(1H,3H-Imidazol-1-yl)-pyrimidine tetrachloridecobaltate (7). A 0.01 M solution of 2-(1H-imidazol-1-yl)-pyrimidine (5 ml) was added to 1 ml of 0.1 M solution of $CoCl_2 \cdot 6H_2O$. The resulting solution was partially evaporated warming at 40 °C during 3 h. Few suitable crystals for X-ray diffraction were grown after several weeks. IR (cm^{-1}): 1628s, 1588s, 1566m, 1528s, 1422s, 1355m, 1129m, 1043m, 966w, 836w, 791m, 753m, 735w, 635m, 509w, 478w.

4.3. X-ray crystallography

X-ray diffraction data were collected in an Enraf-Nonius CAD4 diffractometer with graphite monochromated Mo- $K\alpha$ radiation ($\lambda=0.71073$ Å). Absorption was corrected either with DIFABS or Gaussian quadrature. Structure solution and refinement were performed with SIR2004 and SHELXL97 as included in the WinGX program suite. Non-hydrogen atoms were refined anisotropically. Hydrogen atoms were located in the Fourier difference maps in all cases but 4, where H-atoms were introduced in calculated positions and refined in the riding atom. Details are given in Table 1. The CCDC reference numbers for compounds 1–7 are 845914–845920.

4.4. Computational details

All calculations were carried out using the TURBOMOLE version 5.9²⁶ using the RI-MP2/def2-TZVP level of theory. The RI-MP2 method is considerably faster than MP2 itself and geometries are almost identical for both methods.²⁷ We have used the crystallographic coordinates for the calculations in order to estimate the

contributions of the non-covalent interactions observed in the solid state. Other possible conformations of the crystal fragments have not been considered because the ultimate aim of this study is to analyze the binding properties of the non-covalent interaction in the geometry that they have in the solid state. This approximation has been successfully used by some of us²⁸ and others²⁹ to evaluate non-covalent interactions in the solid state. The partition of the interaction energies into the individual electrostatic, polarization, dispersion, and repulsion components has been carried out by performing Molecular Interaction Potential with polarization (MIPp),¹⁹ which is an improved generalization of the Molecular Electrostatic Potential (MEP) where three terms contribute to the interaction energy, (i) an electrostatic term identical to the MEP,³⁰ (ii) a classical dispersion–repulsion term, and (iii) a polarization term derived from perturbation theory.³¹ The MIPp calculations have been performed by means of the MOPETE-98 program.³² To analyze the intermolecular interactions, the Atoms-In-Molecules (AIM) theory was employed.³³ AIM is based upon those critical points where the gradient of the density, $\nabla\rho$, vanishes. Such points are classified by the curvature of the electron density, for example, a bond critical point has one positive curvature (in the internuclear direction) and two negative ones (perpendicular to the bond). Two bonded atoms are then connected with a bond path through the bond critical point. The properties evaluated at such bond critical points characterize the bonding interactions. They have been widely used to study a great variety of molecular interactions.³⁴

Acknowledgements

We thank CONSOLIDER-Ingenio 2010 (CSD2010-0065) and the MICINN of Spain (project CTQ2008-00841/BQU, FEDER funds) for financial support. C.E. thanks the MICINN of Spain for a fellowship. We thank the CESCA for computational facilities.

Supplementary data

The supplementary file includes a more detailed description of the crystal packing characteristics of compounds 1–7 and the calculation of the Hirshfeld surfaces of the compounds. Supplementary data related to this article can be found online at doi:10.1016/j.tet.2012.01.023.

References and notes

- (a) Karlin, K. D.; Cruse, R. W.; Gultneh, Y.; Farooq, A.; Hayes, J. C.; Zubieta, J. J. *Am. Chem. Soc.* **1987**, *109*, 2668; (b) Karlin, K. D.; Haka, M. S.; Cruse, R. W.; Gultneh, Y. *J. Am. Chem. Soc.* **1985**, *107*, 5828; (c) Kitajima, N.; Koda, T.; Hashimoto, S.; Kitagawa, T.; Moro-oka, Y. *J. Am. Chem. Soc.* **1991**, *113*, 5664; (d) Kitajima, N.; Fujisawa, K.; Fujimoto, C.; Moro-oka, Y.; Hashimoto, S.; Kitagawa, T.; Toriumi, K.; Tatsumi, K.; Nakamura, A. *J. Am. Chem. Soc.* **1992**, *114*, 1277.
- (a) Lai, S. W.; Cheung, T. C.; Chan, M. C. W.; Cheung, K. K.; Peng, S. M.; Che, C. M. *Inorg. Chem.* **2000**, *39*, 255; (b) Ghiladi, R. A.; Ju, T. D.; Kretzer, R. M.; Moenne-Loccoz, P.; Woods, A. S.; Cotter, R. J.; Karlin, K. D. *J. Inorg. Biochem.* **1999**, *74*, 140; (c) Sorrell, T. N.; Garrity, M. L. *Inorg. Chem.* **1991**, *30*, 210; (d) Casella, L.; Carugo, O.; Gullotti, M.; Doldi, S.; Frassoni, M. *Inorg. Chem.* **1996**, *35*, 1101.
- (a) Volbeda, A.; Hol, W. G. L. *J. Mol. Biol.* **1989**, *209*, 249; (b) Solomon, E. I.; Baldwin, M. J.; Lowery, M. D. *Chem. Rev.* **1992**, *92*, 521; (c) Brudvig, G. M.; Stevens, T. H.; Chan, S. I. *Biochemistry* **1980**, *19*, 5275; (d) Martin, C. T.; Morese, R. H.; Kanne, R. M.; Gray, H. B.; Mamström, B. G.; Chan, S. I. *Biochemistry* **1981**, *20*, 5147.
- (a) Bassani, D. M.; Lehn, J.-M.; Fromm, K.; Fenske, D. *Angew. Chem., Int. Ed.* **1998**, *37*, 2364; (b) Breuning, E.; Ruben, M.; Lehn, J.-M.; Renz, F.; García, Y.; Ksenofontov, V.; Gütlich, Ph.; Wegliuss, E.; Rissanen, K. *Angew. Chem., Int. Ed.* **2000**, *39*, 2504; (c) Funeriu, D. P.; Lehn, J.-M.; Fromm, K. M.; Fenske, D. *Chem.—Eur. J.* **2000**, *6*, 2103.
- (a) Elguero, J.; Guerrero, A.; Gómez de la Torre, F.; de la Hoz, A.; Jalón, F. A.; Manzano, B. R.; Rodríguez, A. *New J. Chem.* **2001**, *25*, 1050; (b) Chirayil, S.; Hedge, V.; Jahng, Y.; Thummel, R. P. *Inorg. Chem.* **1991**, *30*, 2821; (c) Gupta, N.; Grover, N.; Neyhart, G. A.; Singh, P.; Thorp, H. H. *Inorg. Chem.* **1993**, *32*, 310; (d) Gómez de la Torre, F.; de la Hoz, A.; Jalón, F. A.; Manzano, B. R.; Otero, A.; Rodríguez, A. M.; Rodríguez-Pérez, M. C.; Echevarría, A.; Elguero, J. *Inorg. Chem.* **1998**, *37*, 6606; (e) Onoa, G. B.; Moreno, V.; Font-Bardia, M.; Solans, X.;

- Pérez, J. M.; Alonso, C. *J. Inorg. Biochem.* **1999**, *205*; (f) Gómez de la Torre, F.; de la Hoz, A.; Jalón, F. A.; Manzano, B. R.; Rodríguez, A. M.; Elguero, J.; Martínez-Ripoll, M. *Inorg. Chem.* **2000**, *39*, 1152; (g) Elguero, J.; Fruchier, A.; de la Hoz, A.; Jalón, F. A.; Manzano, B. R.; Otero, A.; Gómez de la Torre, F. *Chem. Ber.* **1996**, *129*, 589.
6. (a) Meyer, E. A.; Castellano, R. K.; Diederich, F. *Angew. Chem., Int. Ed.* **2003**, *42*, 1210; (b) Schneider, H. *J. Angew. Chem., Int. Ed.* **2009**, *48*, 3924.
7. (a) Desiraju, G. R. *Acc. Chem. Res.* **2002**, *35*, 565; (b) Jeffrey, G. A. *An Introduction to Hydrogen Bonding*; Oxford University: Oxford, 1997; (c) Desiraju, G. R.; Steiner, T. *The Weak Hydrogen Bond in Structural Chemistry, Biology*; Oxford University: Oxford, 1999; (d) Desiraju, G. R. *Nature* **2001**, *412*, 397; (e) Beatty, A. M. *CrystEngComm* **2001**, *1*, 1; (f) Pak, C.; Lee, H. M.; Kim, J. C.; Kim, D.; Kim, K. S. *Struct. Chem.* **2005**, *16*, 187; (g) Lee, H. M.; Suh, S. B.; Lee, J. Y.; Tarakeshwar, P.; Kim, K. S. *J. Chem. Phys.* **2000**, *112*, 9759; (h) Hong, B. H.; Lee, J. Y.; Lee, C.-W.; Kim, J. C.; Bae, S. C.; Kim, K. S. *J. Am. Chem. Soc.* **2001**, *123*, 10748; (i) Steiner, T. *Angew. Chem., Int. Ed.* **2002**, *41*, 48.
8. (a) Hunter, C. A.; Sanders, J. K. M. *J. Am. Chem. Soc.* **1990**, *112*, 5525; (b) Burley, S. K.; Petsko, G. A. *Science* **1985**, *229*, 23; (c) Kim, K. S.; Tarakeshwar, P.; Lee, J. Y. *Chem. Rev.* **2000**, *100*, 4145; (d) Lee, E. C.; Kim, D.; Jurecka, P.; Tarakeshwar, P.; Hobza, P.; Kim, K. S. *J. Phys. Chem. A* **2007**, *111*, 3446; (e) Singh, N. J.; Min, S. K.; Kim, D. Y.; Kim, K. S. *J. Chem. Theory Comput.* **2009**, *5*, 515; (f) Janiak, C. *J. Chem. Soc., Dalton Trans.* **2000**, 3885.
9. (a) Ma, J. C.; Dougherty, D. A. *Chem. Rev.* **1997**, *97*, 1303; (b) Kim, D.; Hu, S.; Tarakeshwar, P.; Kim, K. S.; Lisy, J. M. *J. Phys. Chem. A* **2003**, *107*, 1228; (c) Kim, K. S.; Lee, J. Y.; Lee, S. J.; Ha, T.-K.; Kim, D. H. *J. Am. Chem. Soc.* **1994**, *116*, 7399.
10. (a) Nishio, M.; Hirota, M.; Umezawa, Y. *The C–H/π Interaction: Evidence, Nature, Consequences*; Wiley-VCH: New York, NY, 1998; (b) Nishio, M. *CrystEngComm* **2004**, *6*, 130; (c) Kim, K. S.; Tarakeshwar, P.; Lee, J. Y. *J. Am. Chem. Soc.* **2001**, *123*, 3323.
11. (a) Frontera, A.; Gamez, P.; Mascal, M.; Mooibroek, T.; Reedijk, J. *Angew. Chem., Int. Ed.* **2011**, *50*, 9564; (b) Frontera, A.; Quiñero, D.; Deyà, P. M. *WIREs: Comput. Mol. Sci.* **2011**, *1*, 440; (c) Quiñero, D.; Garau, C.; Rotger, C.; Frontera, A.; Ballester, P.; Costa, A.; Deyà, P. M. *Angew. Chem., Int. Ed.* **2002**, *41*, 3389; (d) Alkorta, I.; Rozas, I.; Elguero, J. *J. Am. Chem. Soc.* **2002**, *124*, 8593; (e) Mascal, M.; Armstrong, A.; Bartberger, M. *J. Am. Chem. Soc.* **2002**, *124*, 6274; (f) Mascal, M. *Angew. Chem., Int. Ed.* **2006**, *45*, 2890; (g) Frontera, A.; Saczewski, F.; Gdaniec, M.; Dziemidowicz-Borys, E.; Kurland, A.; Deyà, P. M.; Quiñero, D.; Garau, C. *Chem.—Eur. J.* **2005**, *11*, 6560.
12. (a) Gil-Ramirez, G.; Escudero-Adan, E. C.; Benet-Buchholz, J.; Ballester, P. *Angew. Chem., Int. Ed.* **2008**, *47*, 4114; (b) Mooibroek, T. J.; Black, C. A.; Gamez, P.; Reedijk, J. *Cryst. Growth Des.* **2008**, *8*, 1082; (c) Kim, D.; Tarakeshwar, P.; Kim, K. S. *J. Phys. Chem. A* **2004**, *108*, 1250; (d) Kim, D.; Lee, E. C.; Kim, K. S.; Tarakeshwar, P. *J. Phys. Chem. A* **2007**, *111*, 7980; (e) Kim, D. Y.; Singh, N. J.; Lee, J. W.; Kim, K. S. *J. Chem. Theory Comput.* **2008**, *4*, 1162; (f) Kim, D. Y.; Singh, N. J.; Kim, K. S. *J. Chem. Theory Comput.* **2008**, *4*, 1401; (g) Gamez, P.; Mooibroek, T. J.; Teat, S. J.; Reedijk, J. *Acc. Chem. Res.* **2007**, *40*, 435; (h) Schottel, B. L.; Chifotides, H. T.; Dunbar, K. R. *Chem. Soc. Rev.* **2008**, *37*, 68; (i) Hay, B. P.; Bryantsev, V. S. *Chem. Commun.* **2008**, 2417; (j) Götz, R. J.; Robertazzi, A.; Mutikainen, I.; Turpeinen, U.; Gamez, P.; Reedijk, J. *Chem. Commun.* **2008**, 3384; (k) Gural'skiy, I. A.; Solntev, P. V.; Krautscheid, H.; Domasevitch, K. V. *Chem. Commun.* **2006**, 4808; (l) Domasevitch, K. V.; Solntev, P. V.; Gural'skiy, I. A.; Krautscheid, H.; Rusanov, E. B.; Chernega, A. N.; Howard, J. A. K. *Dalton Trans.* **2007**, 3893.
13. (a) Mareda, J.; Matile, S. *Chem.—Eur. J.* **2008**, *15*, 28; (b) Gorteau, V.; Bollot, G.; Mareda, J.; Perez-Velasco, A.; Matile, S. *J. Am. Chem. Soc.* **2006**, *128*, 14788; (c) Gorteau, V.; Bollot, G.; Mareda, J.; Matile, S. *Org. Biomol. Chem.* **2007**, *5*, 3000; (d) Gorteau, V.; Julliard, M. D.; Matile, S. *J. Membr. Sci.* **2008**, *321*, 37; (e) Perez-Velasco, A.; Gorteau, V.; Matile, S. *Angew. Chem.* **2008**, *120*, 935; (f) Dawson, R. E.; Hennig, A.; Weimann, D. P.; Emery, D.; Ravikumar, V.; Montenegro, J.; Takeuchil, T.; Gabutti, S.; Mayor, M.; Mareda, J.; Schalley, C. A.; Matile, S. *Nat. Chem.* **2010**, *2*, 533.
14. (a) Estarellas, C.; Frontera, A.; Quiñero, D.; Deyà, P. M. *Angew. Chem., Int. Ed.* **2011**, *50*, 415; (b) Estarellas, C.; Frontera, A.; Quiñero, D.; Deyà, P. M. *Chem.—Asian J.* **2011**, *6*, 2316.
15. Mooibroek, T. J.; Gamez, P.; Reedijk, J. *CrystEngComm* **2008**, *10*, 1501.
16. (a) Egli, M.; Sarkhel, S. *Acc. Chem. Res.* **2007**, *40*, 197; (b) Egli, M.; Gessner, R. V. *Proc. Natl. Acad. Sci. U.S.A.* **1995**, *92*, 180; (c) Sarkhel, S.; Rich, A.; Egli, M. *J. Am. Chem. Soc.* **2003**, *125*, 8998.
17. Calabrese, J. C.; Jordan, D. B.; Boodhoo, A.; Sariaslani, S.; Vannelli, T. *Biochemistry* **2004**, *43*, 11403.
18. (a) Garcia-Raso, A.; Alberti, F. M.; Fiol, J. J.; Tasada, A.; Barceló-Oliver, M.; Molins, E.; Estarellas, C.; Frontera, A.; Quiñero, D.; Deyà, P. M. *Cryst. Growth Des.* **2009**, *9*, 2363; (b) Garcia-Raso, A.; Alberti, F. M.; Fiol, J. J.; Tasada, A.; Barceló-Oliver, M.; Molins, E.; Escudero, D.; Frontera, A.; Quiñero, D.; Deyà, P. M. *Eur. J. Org. Chem.* **2007**, 5821; (c) Garcia-Raso, A.; Alberti, F. M.; Fiol, J. J.; Tasada, A.; Barceló-Oliver, M.; Molins, E.; Escudero, D.; Frontera, A.; Quiñero, D.; Deyà, P. M. *Inorg. Chem.* **2007**, *46*, 10724.
19. Luque, F. J.; Orozco, M. *J. Comput. Chem.* **1998**, *19*, 866.
20. (a) Hernández, B.; Orozco, M.; Luque, F. J. *J. Comput.-Aided Mol. Des.* **1997**, *11*, 153; (b) Luque, F. J.; Orozco, M. *J. Chem. Soc., Perkin Trans. 2* **1993**, 683; (c) Quiñero, D.; Frontera, A.; Suñer, G. A.; Morey, J.; Costa, A.; Ballester, P.; Deyà, P. M. *Chem. Phys. Lett.* **2000**, *326*, 247; (d) Quiñero, D.; Frontera, A.; Garau, C.; Ballester, P.; Costa, A.; Deyà, P. M. *ChemPhysChem* **2006**, *7*, 2487; (e) Garau, C.; Quiñero, D.; Frontera, A.; Ballester, P.; Costa, A.; Deyà, P. M. *J. Phys. Chem. A* **2005**, *41*, 9341; (f) Garau, C.; Quiñero, D.; Frontera, A.; Ballester, P.; Costa, A.; Deyà, P. M. *Org. Lett.* **2003**, *5*, 2227; (g) Garau, C.; Quiñero, D.; Frontera, A.; Ballester, P.; Costa, A.; Deyà, P. M. *Chem. Phys. Lett.* **2003**, *370*, 7; (h) Garau, C.; Frontera, A.; Ballester, P.; Quiñero, D.; Costa, A.; Deyà, P. M. *Eur. J. Org. Chem.* **2005**, 179.
21. (a) Cherg, Y. J. *Tetrahedron* **2002**, *58*, 887; (b) Xie, Y.-X.; Pi, S.-F.; Wang, J.; Yin, D.-L.; Li, J.-H. *J. Org. Chem.* **2006**, *71*, 8324.
22. Boldog, I.; Daran, J.-C.; Chernega, A. N.; Rusanov, E. B.; Krautscheid, H.; Domasevitch, K. V. *Cryst. Growth Des.* **2009**, *9*, 2895.
23. Brunet, E.; Juanes, O.; Sedano, R.; Rodríguez-Ubis, J. C. *Tetrahedron Lett.* **2007**, *48*, 1091.
24. Thiruvalluvar, A.; Subramanyam, M.; Kalluraya, B.; Lingappa, B. *Acta Crystallogr.* **2007**, *E63*, o3362.
25. Mandal, T. N.; Roy, S.; Barik, A. K.; Gupta, S.; Butcher, R. J.; Kar, S. K. *Polyhedron* **2008**, *27*, 3267.
26. Ahlrichs, R.; Bär, M.; Häser, M.; Horn, H.; Kölmel, C. *Chem. Phys. Lett.* **1989**, *162*, 165.
27. Frontera, A.; Quiñero, D.; Garau, C.; Ballester, P.; Costa, A.; Deyà, P. M. *J. Phys. Chem. A* **2005**, *109*, 4632.
28. (a) Das, A.; Choudhury, S. R.; Estarellas, C.; Dey, B.; Frontera, A.; Hemming, J.; Helliwell, M.; Gamez, P.; Mukhopadhyay, S. *CrystEngComm* **2011**, *13*, 4519; (b) Seth, S. K.; Saha, I.; Estarellas, C.; Frontera, A.; Kar, T.; Mukhopadhyay, S. *Cryst. Growth Des.* **2011**, *11*, 3250; (c) Biswas, R.; Drew, M. G. B.; Estarellas, C.; Frontera, A.; Ghosh, A. *Eur. J. Inorg. Chem.* **2011**, 2558; (d) Barceló-Oliver, M.; Estarellas, C.; Terrón, A.; Garcia-Raso, A.; Frontera, A. *Chem. Commun.* **2011**, 4646; (e) Biswas, S.; Naiya, S.; Drew, M. G. B.; Estarellas, C.; Frontera, A.; Ghosh, A. *Inorg. Chim. Acta* **2011**, *366*, 219; (f) Barceló-Oliver, M.; Estarellas, C.; Garcia-Raso, A.; Terrón, A.; Frontera, A.; Quiñero, D.; Mata, I.; Molins, E.; Deyà, P. M. *CrystEngComm* **2010**, *12*, 3758; (g) Naiya, S.; Drew, M. G. B.; Estarellas, C.; Frontera, A.; Ghosh, A. *Inorg. Chim. Acta* **2010**, *363*, 3904; (h) Garcia-Raso, A.; Alberti, F. M.; Fiol, J. J.; Lagos, Y.; Torres, M.; Molins, E.; Mata, I.; Estarellas, C.; Frontera, A.; Quiñero, D.; Deyà, P. M. *Eur. J. Org. Chem.* **2010**, 5171.
29. (a) Choudhury, S. R.; Dey, B.; Das, S.; Robertazzi, A. o; Jana, A. D.; Chen, C. Y.; Lee, H. M.; Gamez, P.; Mukhopadhyay, S. *Dalton Trans.* **2009**, 38, 7617; (b) de Hoog, P.; Robertazzi, A.; Mutikainen, I.; Turpeinen, U.; Gamez, P.; Reedijk, J. *Eur. J. Inorg. Chem.* **2009**, 2684; (c) Goetz, R. J.; Robertazzi, A.; Mutikainen, I.; Turpeinen, U.; Gamez, P.; Reedijk, J. *Chem. Commun.* **2008**, 3384.
30. Scrocco, E.; Tomasi, J. *Top. Curr. Chem.* **1973**, *42*, 95.
31. Francl, M. M. *J. Phys. Chem.* **1985**, *89*, 428.
32. Luque, J. F.; Orozco, M. *MOPETE-98 Computer Program*; Universitat de Barcelona: Barcelona, 1998.
33. Bader, R. F. W. *Atoms in Molecules-A Quantum Theory*; Oxford University: Oxford, 1990.
34. (a) Bader, R. F. W. *Chem. Rev.* **1991**, *91*, 893; (b) Grabowski, S. J.; Pfitzner, A.; Zabel, M.; Dubis, A. T.; Palusiak, M. *J. Phys. Chem. B* **2004**, *108*, 1831; (c) Vila, A.; Mosquera, R. A. *THEOCHEM* **2001**, *546*, 63; (d) Chopra, D.; Cameron, T. S.; Ferrara, J. D.; Guru Row, T. N. *J. Phys. Chem. A* **2006**, *110*, 10465.